

## IMPLEMENTATION AND RELIABILITY ISSUES WITH LEAD-FREE SOLDERS

Christopher Hunt  
National Physical Laboratory  
Teddington, United Kingdom  
chris.hunt@npl.co.uk

### ABSTRACT

Manufacturing high reliability lead-free circuit assemblies is challenging, and understanding the pitfalls and knowing material properties is clearly desirable. This paper will address a wide range of issues, which include material and processing properties. Examples of these phenomena include: copper dissolution, tin whisker mitigation, PTH reliability, measuring solder joint reliability, conformal coating protection, and tin pest.

### MEASURING COPPER DISSOLUTION

PCB metallised interconnect generally comprises exposed copper, and during the assembly process this copper will be exposed to molten solder. Since the major constituent of any solder is tin, dissolution of the copper will occur. This is a significant issue for product reliability, since copper can be eroded from specific sites during certain soldering operations to the extent that electrical continuity is lost or reliability compromised.

The advent of lead-free soldering has resulted in the introduction of a number of high tin solder alloys, which for selective soldering applications, typically means solders with melting temperatures in excess of 220°C. The higher melting points of the lead-free alloys also dictate higher processing temperatures, and usually higher contact times, as the components take longer to heat up to the higher processing temperature. The copper dissolution process is temperature and solder alloy dependent. The solubility of copper in the new lead free alloys with tin compositions of at least 95% tin is potentially higher than that of tin-lead solder. Hence, the higher temperature and solubility effects can significantly increase the risk of damaging copper due to dissolution. Exposed surface copper can be removed, disconnecting the land from the track.

The formation of a solder joint during soldering requires a reaction between the solder and the metallisation of the substrate. This reaction involves a dissolution process, which occurs through an intermediate phase of an intermetallic that forms at the interface. The intermetallic itself is soluble in molten solder, and hence the intermetallic substrate interface proceeds into the substrate with time. The nature of this intermetallic and its thickness will be significant in controlling the overall copper dissolution process. A number of alloys are now available where additions significantly below 1% affect a number of

material properties, of which the solubility of copper is an important parameter.

There are numerous interacting factors affecting dissolution which include: copper type, alloy composition, fluidity, temperature, flow rate, intermetallic formation, and geometry issues. Therefore there is a requirement to assess the susceptibility of a PCA to dissolution to a specific set of variables. Interaction of variables is important, and temperature is one of the most complicated terms, effecting parameters such as fluidity, solubility and intermetallic formation.

To characterise copper dissolution in assembly production there is a need to be able to measure the dissolution rate. Typically this is not easily achieved since inspection of a PCA will only reveal whether copper is present or not, not how thick it is. Hence this project has devised a simple approach that can be used to characterise the dissolution rate for a given soldering process.

### Materials and Experimental Set Up

One of the aims of this study is the development of a simple testing method that can be universally employed for evaluating a number of variables. For this study a typical PCB construction as used in industry was utilised, using a specific design of copper pad. This is shown in Figure 1 The PCB was a 2.5 mm thick FR4, with 10 copper test pads, further details of this are given in reference[1]. The test pads can also be accessed from the bottom side through a hole. The topside shows small dimples where the copper is unsupported, and the hole can be clearly seen from the top view. Another requirement of the testing method is an automated detection of the dissolution time. A contact for the timing probe can easily be inserted into the hole to sense when the solder penetrates the copper foil and contacts the pin. The soldering machine used for the tests was an ACE Automated Soldering Machine - KISS 102, using a travelling mini-solder fountain. Alloys with composition close to those commercially available were tested here. The alloy composition was analysed using inductively coupled plasma – atomic emission spectroscopy (ICP-AES), and the results are shown in Table 1.

### Experimental Results

A flow rate of 1.35 cm<sup>3</sup>/s was selected for the tests, as it was found to work well with all alloys and corresponded to a typical solder fountain profile, as suggested by the selective

soldering machine manufacturer. This achieved the necessary solder fountain height, without being too turbulent. The correct pump speed to apply during the dissolution tests could be calculated from the flow rate/pump speed relationship using linear interpolation. The dissolution rate of the alloys tested at 255, 275 and 300 °C are shown in Figure 2.

### Discussion

Controlling the flow rate during the test was seen to be important step to insure a better comparison between the different solder alloys. The dissolution rate, which was found to increase linearly with temperature, varied between the different alloys. This demonstrated the role that the composition of the alloys plays in this phenomenon. It was observed that the SnPb alloy was not the alloy with the lowest dissolution rate within the temperature interval used here (see Figure 2).

The slope of the dissolution rate curves of Alloys A, B, C, F, H and SnPb were very similar. The curves for alloys D, E and SnAg had a higher slope, indicating a higher dependence of the dissolution rate with temperature. The alloys that presented the highest copper dissolution rates in the commonly used for soldering temperature range 275-300 °C, were alloys E, G and SnAg. Finding SnAg in this group was expected, because of the high solubility of Cu in Sn<sub>3.5</sub>Ag [2]. Alloys E and G are very similar in composition (see Table 1), so a similar behaviour was to be expected. However, it is not clear why their copper dissolution behaviour was poor. The relatively high Cu content should have a positive effect compared to SnAg, but this was not observed. The alloys that showed the lowest copper dissolution rates were alloys A, D and H. It is likely that the good performance of alloys D and H is due to their Ni content. In the presence of Ni, complex Ni-based IMCs tend to form instead of Cu<sub>6</sub>Sn<sub>5</sub>. The Ni IMC acts as a superior barrier, protecting the underlying copper [3].

It was previously observed that the characteristics of the intermetallic layer play an important role in the dissolution rate. Cross sections of the tested samples were made and observed using an SEM, in order to measure the IMC thickness. In general it was found that the thicker the intermetallic layer, the smaller the copper dissolution rate, as shown in Figure 3. This is consistent with the intermetallic acting as a barrier for copper diffusion, and explains why alloy A shows the lowest dissolution rate of copper. Variations in intermetallic microstructure may also influence the dissolution process and reflect the range of results, but further research would be necessary to confirm this.

### Summary

The various factors that influence the dissolution of copper in molten solder were investigated and the important parameters were found to be: temperature, solder composition and flow rate.

A method was developed for comparing the dissolution rate of copper with different solder alloys. The method developed here, presents many advantages. First of all, the detection of the dissolution time was instrumented, hence improving repeatability. This method removes the need for cross sectioning to measure the dissolution rate, and hence the measurement process is very quick, and potentially real time within the machine setup process. Ten copper pads can be tested automatically in rapid succession, insuring constant conditions and repeatability of the results. The procedure is also very flexible and can be adapted and used for different types of soldering machines and providing the same conditions are used, comparable results should be obtainable.

These features make the procedure described here an important tool for future testing in the copper dissolution area. In particular studies that investigate the effect of different copper types could benefit from the flexibility and ability to obtain a large number of results in a short period of time.

### TIN WHISKER MITIGATION

A tin whisker can cause catastrophic failure of electronics, yet there are no guaranteed whisker free tin finishes available. The whisker formation process is not fully understood, although there must be compressive stresses in the tin layer to drive the whisker formation. This is a significant issue since the component industry makes extensive use of tin finishes, and hence there is considerable interest from high reliability users to mitigate against whiskering. The use of conformal coatings has been suggested as a means of controlling whisker growth, either by inhibiting the initiation of growth or by preventing whisker growths shorting between adjacent conductors [4-8]. Work carried out by Boeing on commercially available coatings has shown suppression of tin whiskers when compared to the uncoated controls [6,7]. However, all of the commercial coatings were eventually penetrated by whiskers, indicating that these coatings cannot be depended on as a foolproof mitigation strategy.

A test vehicle design that resembles a parallel plate capacitor has been developed. This test vehicle allows whisker growth to be monitored over a large area using electrical detection [9]. The plates are plated with a chemistry that by controlling the tin thickness will either whisker in a few days when held at room temperature, or will not whisker in at least 6 months. Following plating, samples are conformally coated within 48 hrs, and then folded up to form the parallel plate assembly.

Four different styles of test vehicle can be fabricated as detailed below and shown in Figure 4, to investigate whisker growth in different areas:

- Type 1 (whisker out) vehicles were designed to monitor for whisker growth from beneath a conformal coating. The plates to be coated were electroplated with thin Sn (<2µm) to generate whiskers. The uncoated plates were

electroplated with thick Sn ( $>10\mu\text{m}$ ) to act as a detector plate.

- Type 2 (whisker in) vehicles were designed to monitor for whisker growth through a conformal coating from an external uncoated source. The plates to be coated were electroplated with thick Sn ( $>10\mu\text{m}$ ) to act as a detector plate. The uncoated plates were electroplated with thin Sn ( $<2\mu\text{m}$ ) to generate whiskers.
- Type 3 (whisker in/out) were designed to monitor for whisker growth out from under a conformal coating and then back through an adjacent coating. Both plates to be coated were electroplated with thin Sn ( $<2\mu\text{m}$ ) to generate whiskers.
- Type 4, designed as control samples. The plates are left uncoated and electroplated with thin Sn ( $<2\mu\text{m}$ ) to generate whiskers.

In the preliminary investigation three coating types were investigated: paraxylene, polyurethane and acrylic. The paraxylene coating proved to resist any whisker growth, even when it had been coated over whiskers that had just started to form. The polyurethane did resist whiskers growing out from underneath, but whisker were able to penetrate the coating. The acrylic coating was the least robust, it allowed more whiskers to penetrate sooner and a whisker did penetrate out of the coating.

So the technique was able to determine the relative ability of a conformal coating to mitigate against tin whisker growth. All the control samples without conformal coatings developed whiskers of sufficient length ( $>250\mu\text{m}$ ) to cause electrical shorts. The control samples all exhibited electrical shorts within 14 days, some within as few as 3 days, allowing for a relatively rapid i.e. less than 12 week evaluation of the tin whisker mitigation benefits of conformal coatings. Longer term testing would be required to ensure the coated samples remained whisker free. Future publications of this study will consider a larger range of coatings.

#### **PLATED THROUGH HOLE RELIABILITY**

Lead-free solders are all high tin alloys with significantly higher melting points compared to earlier tin-lead materials. Substrate technology has been developed around reinforced resin materials and increased degradation caused by the associated higher processing temperatures is a possibility. This is compounded by the interconnecting structures being brought into closer proximity as a result of increasing technology advances driven by miniaturisation. An earlier study investigated laminate materials and processing issues [10]. The removal of non-functional pads to facilitate signal routing and improved drilling conditions for high aspect ratio vias, may also affect substrate reliability. The damage caused to a PTH is shown in Figure 5, where barrel cracks can be observed.

The National Physical Laboratory and PWB Interconnect Solutions Inc. have undertaken a joint study [11], following identical test structures through both thermal cycling, with

constant electrical monitoring (event detecting) and Interconnect Stress Testing (IST). The test vehicles included patterns to monitor changes in interconnection spacing (pitch) and also the effect of removing non-functional pads. The failure modes generated with both techniques were similar as were the relative rankings of the effects. Results from thermal cycling are shown in Figure 6, and this Weibull plot clearly shows there is a difference in the performance with and without non-functional pads. The results showed that the removal of non-functional pads tended to improve reliability for high aspect ratio plated through holes in thicker substrates, although increasing interconnection pitch had little effect on failure rate.

The results generated by both thermal cycling and IST showed extremely good correlation, as presented in Figure 7. Failures occurred at a slightly lower number of cycles for IST compared to thermal cycling due to the more stringent failure criteria used in IST of a 10% resistance change. The relative ranking of the level of failures is identical for both the thermal cycling and IST but the results were obtained in very different timescales. IST has been shown to give fast comparable results to thermal cycle testing with constant monitoring, but thermal cycling may be more beneficial if a wider range of experimental parameters (E.g. solder joints) are to be tested simultaneously.

#### **MEASURING SOLDER JOINT RELIABILITY**

One of the main performance criteria for solders relates to the low cycle fatigue performance. Many studies have been performed where circuit assemblies have been thermally cycled and the solder joint performance characterised. At NPL we are attempting to measure the material properties of the solder joint that takes into account size effects, using an approach originally outlined in [12]. This is being achieved using a sample with a single solder joint, as shown in Figure 8. The sample joint height here is  $300\mu\text{m}$ , and hence the intermetallics at the interface are important, and the overall performance is similar to that of a surface mount joint. The sample is mounted in a test machine to measure the stress strain cycle, where the sample temperature can also be controlled. The solder response to this displacement is shown in Figure 9, where the creep and relaxation of the force is presented. The energy lost in increasing cycles of strange range is also presented, showing the increasing size of the hysteresis loop, and the damage accumulated in the solder joint. This approach can be used to determine the lifetime degradation response of the solder joint. In Figure 10 the lifetime results are presented for three isothermal tests for a strain range of  $\pm 0.05$ .

The creep, relaxation and hysteresis behaviour are all extremely important material parameters for comparing solders. These material constants can also be used in modelling, and by comparison with thermal cycling experiments the prediction of lifetime with alternative joint characteristics and various thermal cycle parameters, improved lifetime prediction should be possible.

## CONFORMAL COATING PROTECTION

Coatings are applied to protect electronics from condensation and adventitious contamination effects. There are ranges of basic coating chemistries and these can be modified to control other parameters, such as rheology. An important aspect of coating performance can be evaluated by measuring the electrical resistance at the interface between the coating and substrate using an interdigitated comb pattern. If the electrical pattern to be tested is not a comb pattern but formed using component terminations then coating coverage is also evaluated. Coatings' sensitivity to different contaminants can be evaluated by applying a solution of the contaminant, and allowing it to dry. Subsequent damp heat testing will evaluate the ability of the contaminant to penetrate the coating by measuring a change in the underlying resistance. More details are described in [13-15]. An example from such a study presented in Figure 11 reveals the relative performance.

Coating coverage around component termination edges is a real challenge. In Figure 12 the lack of coating coverage along the termination edge provides a weak site where corrosion can initiate in the damp heat test. The contamination in the presence of moisture and electric bias as facilitated the corrosion process to imitate between terminations across the top of the coating. Hence damp heat testing with resistance monitoring under the coating can utilised to determine the protection capability of a coating.

## TIN PHASE TRANSFORMATION (TIN PEST)

The  $\beta$  phase of tin is stable only down to 13°C. Below that temperature the thermodynamically stable phase is  $\alpha$  tin, more commonly known as tin pest. This phase has gained notoriety because of the catastrophic consequences to the transforming metal. Interest in this subject increased after the transition from tin-lead to lead-free solder, driven by the European RoHS legislation. Lead-free alloys contain from 95 to 99% tin and could potentially be susceptible to the  $\beta/\alpha$  transformation. The transformation takes a long time to occur, months or even years, especially in alloys of Sn. For this reason it is particularly difficult to observe. At NPL a procedure for observing and measuring the transformation based on electrical measurements has been developed [16]. Furthermore a sample preparation technique that considerably accelerates the transformation in alloys is used based on the introduction of a seed.

A seeded sample was prepared by immersing  $5 \pm 0.5$  mg of CdTe powder into 1gm of molten Sn, giving samples typically 40mm long and 1.8mm radius. The sample was solidified in an oxidised steel mould in the shape of a small cylinder, with the inoculated part at one extremity. The second part of this sample consisted of 1gm of a Sn alloy, for example Sn-Cu. The two parts were placed next to each other in the mould and the two parts were fused together, melting the interfacial region, and allowing any dross to appear at the surface and be dispersed. Tweezers were used to gently push the samples together while the interfacial zone was molten. When a joint had been formed the

interfacial zone was kept molten for 5 seconds to allow the diffusion of the alloying element into the pure tin. This generated a gradient in composition between the pure Sn and the alloy. Sn-Cu, Sn-Ag, Sn-Zn, Sn-Ni, Sn-Bi, Sn-In and Sn-Pb hybrid samples were prepared for this study, where the second element added was ~0.4mass%. The seven binary alloys were tested with this procedure and ranked in terms of their propensity to transform. The change in electrical resistance as the transformation proceeded is presented in Figure 13. The typical effect of the transformation on the appearance of a sample before and after the transformation is presented in Figure 14, and this is for SnNi, although they all appear similar.

The acceleration of the incubation/nucleation phase of the transformation is not *expected* to occur in the field. However, this method makes it possible to study the  $\alpha$ -Sn crystal growth in different materials in a reasonable timescale. This study focused on binary alloys; however commercial alloys are also being studied and will be the topic of future publications.

This study has confirmed previous qualitative observations indicating Bi to be the main element for preventing the transformation of tin. Pb, which in previous studies was believed to be as effective as Bi, did not stop the sample from transforming, but just decelerated the process. The transformation speeds of SnAg and SnCu were similar to pure Sn (99.99%).

## CONCLUSIONS

The implementation of the RoHS directive has clearly had a material impact, but in turn the new materials have had a number of processing impacts, namely an increase in the processing temperature during assembly. These changes have been accommodated in high volume consumer markets, but for high reliability and high stress environments the reliability case is not yet proven. Processing issues such as copper dissolution can be solved by machine design modifications and minor elemental modification to the alloys to reduce copper solubility. The PCB substrate is pushed very hard during the multiple higher temperature reflow passes. This can impact on the PTH reliability, can cause delamination and increase susceptibility to CAF. Fatigue of solder, both low and high cycle fatigue, are still areas that are being investigated, and prediction and defining acceleration factors have yet to be defined. Clearly for safety critical equipment a high level of confidence will be required for these acceleration factors. While tin pest remains an issue more of an academic interest, that alloys of tin can transform if nucleated is of concern. The question that needs to be answered is how does nucleation initiate in this system and what are the environmental factors. Tin whiskers remains an ongoing issue as no plated tin finish is guaranteed as whisker free, hence the interest in mitigation strategies and whether coatings can mitigate against a whisker short. The test approach developed here will facilitate coating developments for this purpose. Finally symptomatic of an

increase in electronics reliability across the board there is increasing interest in applying coatings, and the work presented here shows opportunities for improved evaluation techniques for coatings.

#### ACKNOWLEDGMENTS

This work was funded by the UK government out of their National Measurement Office. The author is grateful to the following: Davide Di Maio, Martin Wickham, Ling Zou and Owen Thomas.

#### REFERENCES

- [1] Di Maio, D., Hunt, C.P., (2009), "Measurements of Copper Dissolution in Lead-Free Alloys", NPL Report, MAT 26 ISSN: 1754-2979, National Physical Laboratory, Teddington, UK.
- [2] Yu, D.Q., Wu, C.M.L., Law, C.M.T., Wang, L. and Lai, J.K.L., (2005), "Intermetallic compounds growth between Sn-3.5Ag lead-free solder and copper substrate by dipping method", *Journal of Alloys and Compounds* Vol. 392.
- [3] Izuta, G., Tanabe, T., Suganuma, K., (2007), "Dissolution of Sn-Ag-Cu System Lead-Free Solder", *Soldering & Surface Mount Technology*, Vol. 19 No. 2, pp. 4-11.
- [4] Kadesch, J.S., Leidecker, H.; Effects of Conformal Coat on Tin Whisker Growth; Proceedings of the 37th IMAPS Nordic Conference, September 2000
- [5] Kadesch, J.S., Brusse J.; The Continuing Dangers of Tin Whiskers and Attempts to Control Them with Conformal Coating; NASA EEE Links Newsletter July 2001
- [6] Woodrow, T.; Evaluation of Conformal Coatings as a Tin Whisker Mitigation Strategy; IPC/JEDEC 8th International Conference on Pb-Free Electronic Components and Assemblies, San Jose, CA, April 18-20, 2005
- [7] Woodrow, T.; Evaluation of Conformal Coatings as a Tin Whisker Mitigation Strategy, Part 2; SMTAI, Sept. 2006
- [8] Nishimi, K.; Space Shuttle Program - Tin Whisker Mitigation; Intl. Symposium on Tin Whiskers, Apr. 2007
- [9] Wickham, M., Hunt, C.P., (2008), "Test Method for Measurement of the Propensity for Conformal Coatings to Inhibit Tin Whiskering", NPL Report, MAT 28 ISSN: 1754-2979, National Physical Laboratory, Teddington, UK.
- [10] Wickham, M., Dusek, M., & Hunt, C.P., (2007), "Reliability of Electronic Substrates After Processing at Lead-free Soldering Temperatures", NPL Report, MAT 10 ISSN: 1754-2979, National Physical Laboratory, Teddington, UK.
- [11] Hunt, C.P., and Wickham, M., (National Physical Laboratory), & Birch, W., and Furlong, J., (PWB Interconnect Solutions Inc., Nepean, Canada), The Effect of Functional Pads and Pitch on Via Reliability using Thermal Cycling and Interconnect Stress Testing, APEX 2009, S17-02
- [12] Dusek, M., & Hunt, C.P., (2006), "Test Approach to Isothermal Fatigue Measurements for Lead-free Solders", DEPC-MPR 048, March 2006
- [13] Mensah, A., and Hunt, C.P., "The Role of Permeability and Ion Transport in Conformal Coating Protection", NPL Report DEPC-MPR 032, September 2005
- [14] Zou, L., Hunt, C.P., "Protection Performance of Conformal Coatings in Harsh Environments", DEPC-MPR 054, July 2006
- [15] Zou, L., Hunt, C.P., "Test Method for Conformal Coating Protection Performance of Electronic Assembly in Harsh Environments", DEPC-MPR 060, March 2007
- [16] Di Maio, D., Hunt, C.P., (2008), "Investigation Methods of the  $\beta$  to  $\alpha$  Tin Allotropic Transformation", NPL Report, MAT 21 ISSN: 1754-2979, National Physical Laboratory, Teddington, UK

**Table 1: Composition of the alloys used for the tests (weight %).  
The remaining contribution is from tin**

%	Ag	Bi	Cu	Co	Ni	Pb	Sb
A	0.050	<0.01	0.626	0.030	<0.01	0.040	0.020
B	0.024	<0.01	0.510	0.081	<0.01	0.005	0.008
C	2.520	<0.01	0.748	<0.01	<0.01	0.030	0.700
D	<0.01	<0.01	0.660	<0.01	0.050	0.018	0.017
E	0.338	<0.01	0.594	<0.01	<0.01	0.006	0.011
F	3.700	<0.01	0.730	<0.01	<0.01	0.015	0.017
G	0.301	0.090	0.682	<0.01	<0.01	0.016	0.017
H	0.210	<0.01	0.690	<0.01	0.040	0.030	0.010
SnPb	<0.01	<0.01	<0.01	<0.01	<0.01	60.340	0.010
SnAg	4.100	<0.01	<0.01	<0.01	<0.01	0.012	0.018

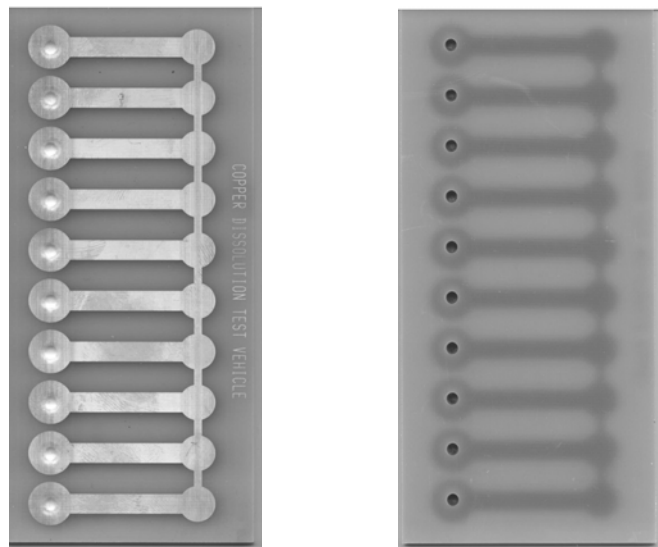


**Figure1: The bottom and top side of the PCB (left and right respectively) coupon used for the tests.  
The holes on the bottom side correspond to the unsupported part of the copper pads seen on the top side.**

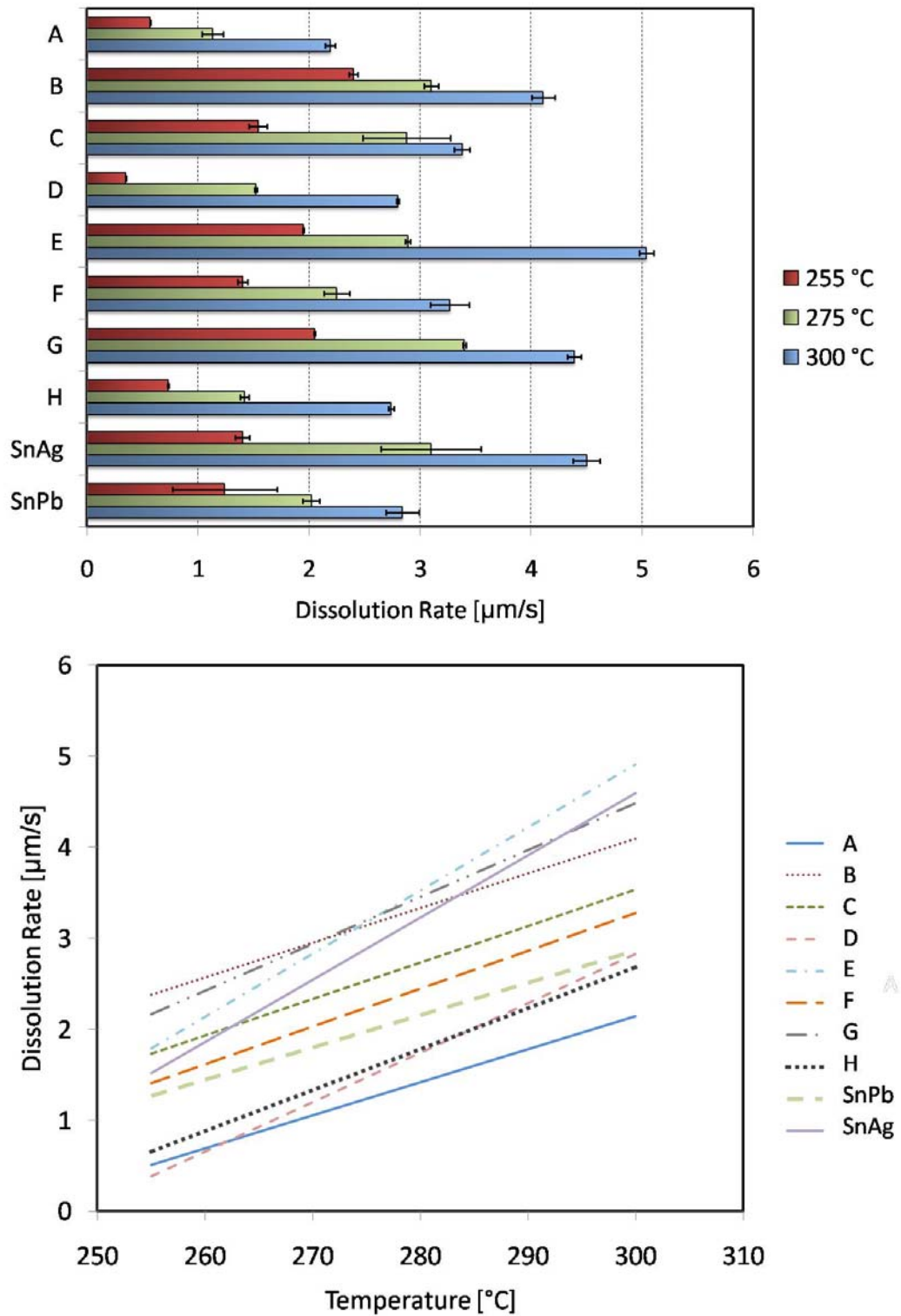


Figure 2: The dissolution rate of the alloys at the temperatures of 255, 275 and 300 °C.

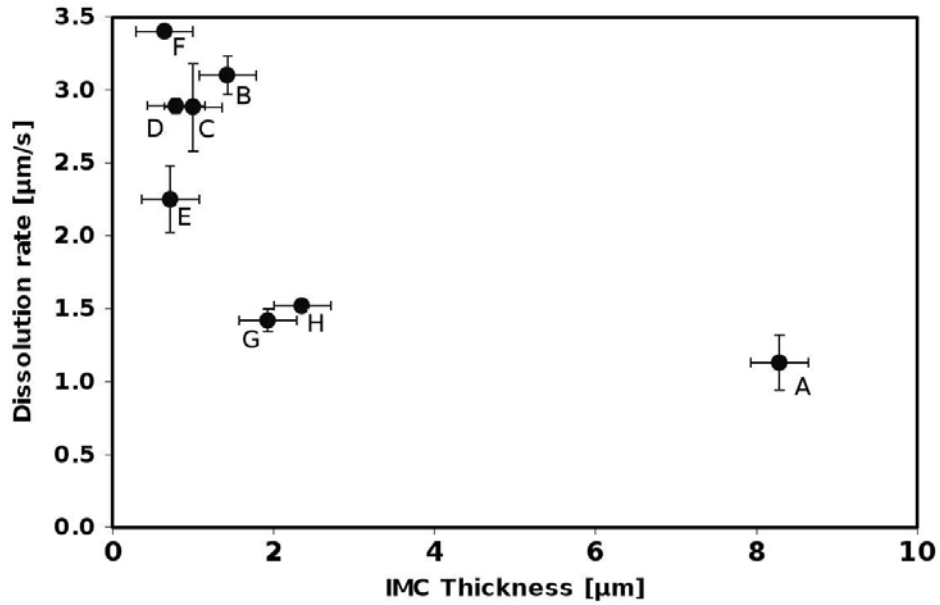


Figure 3: Dissolution rate of copper in the solder alloys and IMC thickness relationship (275 °C).

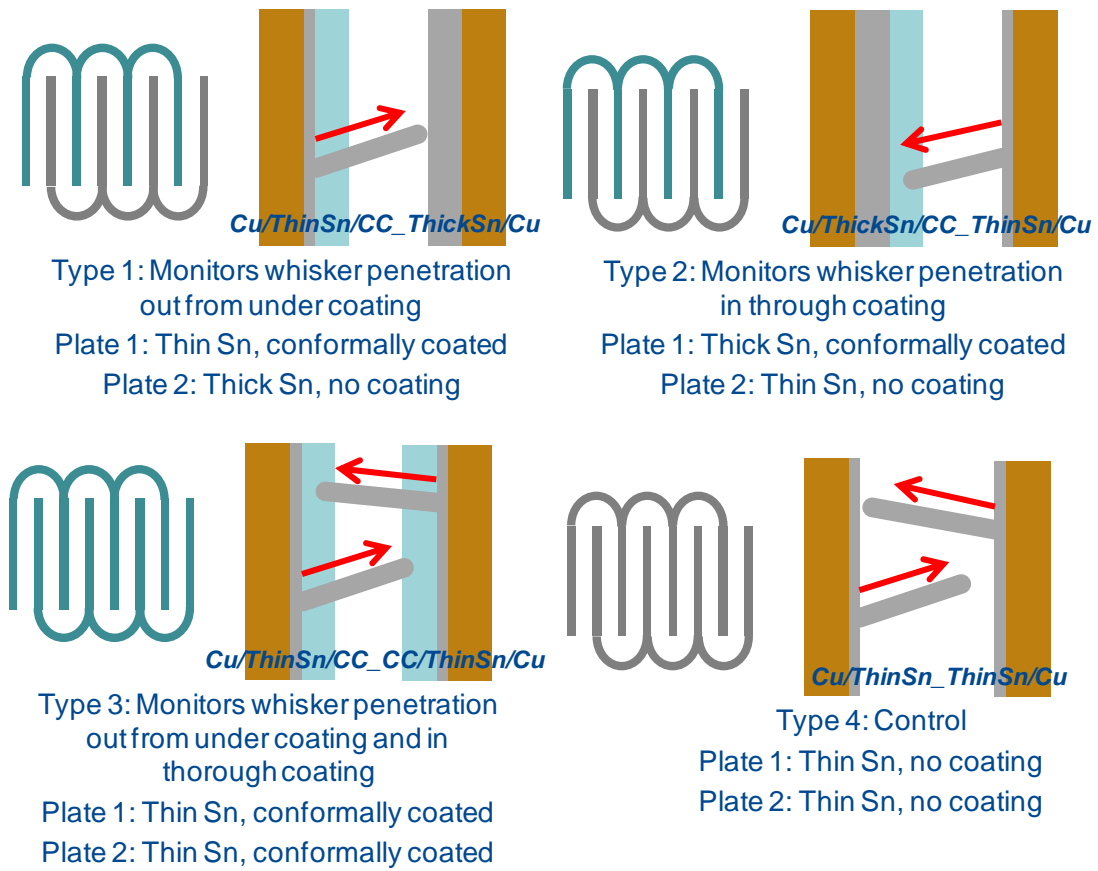


Figure 4: Schematics of the four types of test vehicle arrangement for tin whisker mitigation evaluation



Figure 5: Microsection of via with failure in region where non-functional pads have been retained.

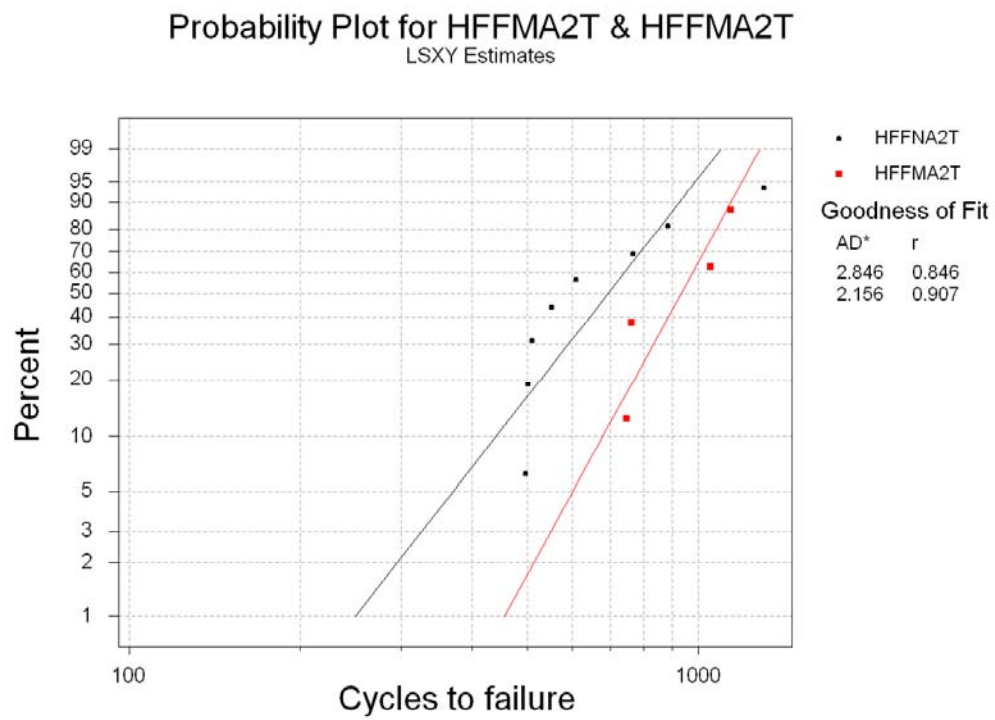


Figure 6: Weibull plot of thermal cycle failures for HFFNA2T (non-function pads included) and HFFMA2T (non-functional pads removed)

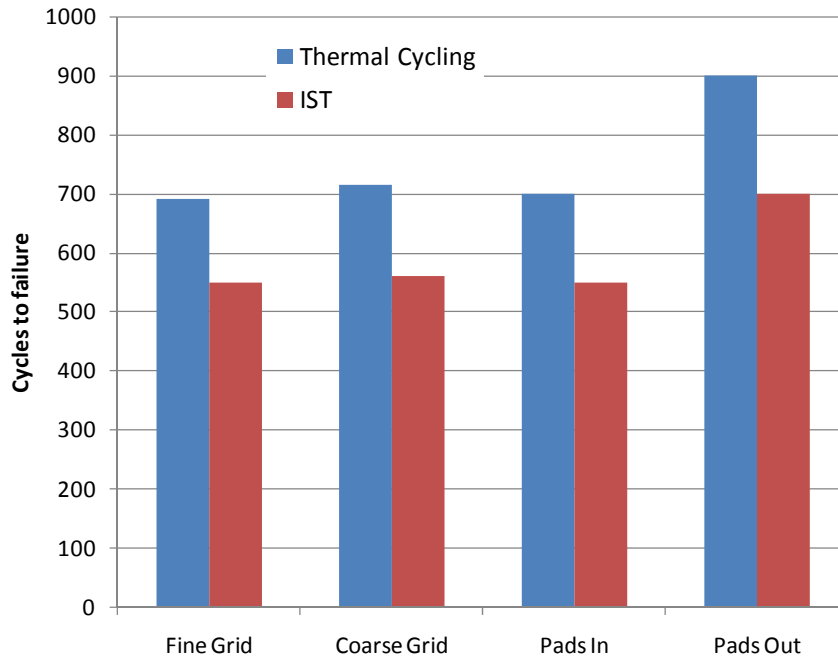


Figure 7: Comparison of number of cycles to 50% failures for thermal cycling and IST

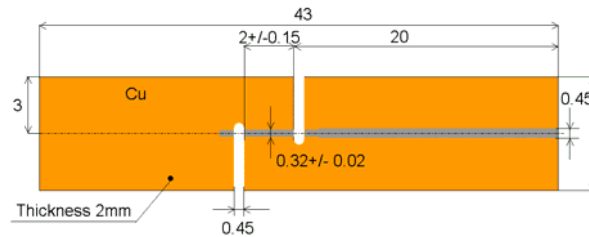


Figure 8: Single solder joint fatigue sample

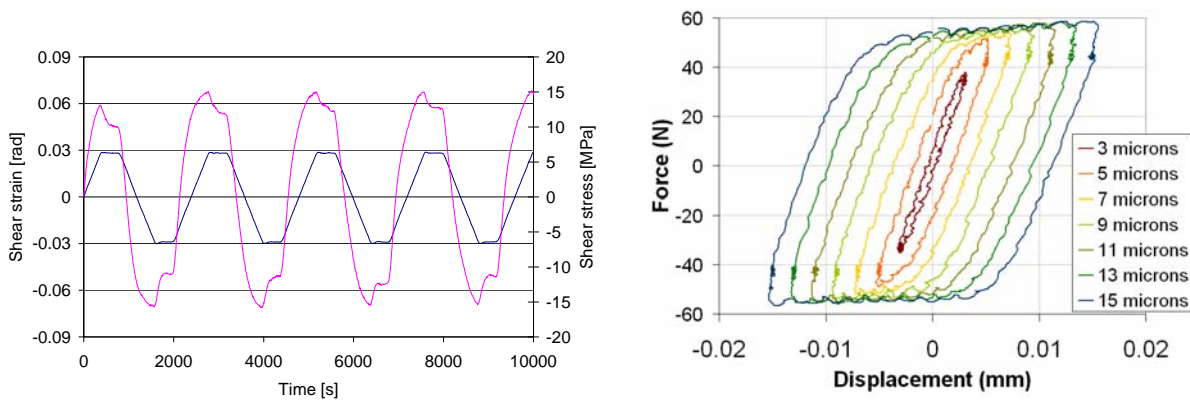


Figure 9: (a) Shows the stress response to the imposed strain profile, where the creep and relaxation can be clearly seen. (b) Shows the increasing hysteresis loop, and the energy loss in the solder joint during the cycle.

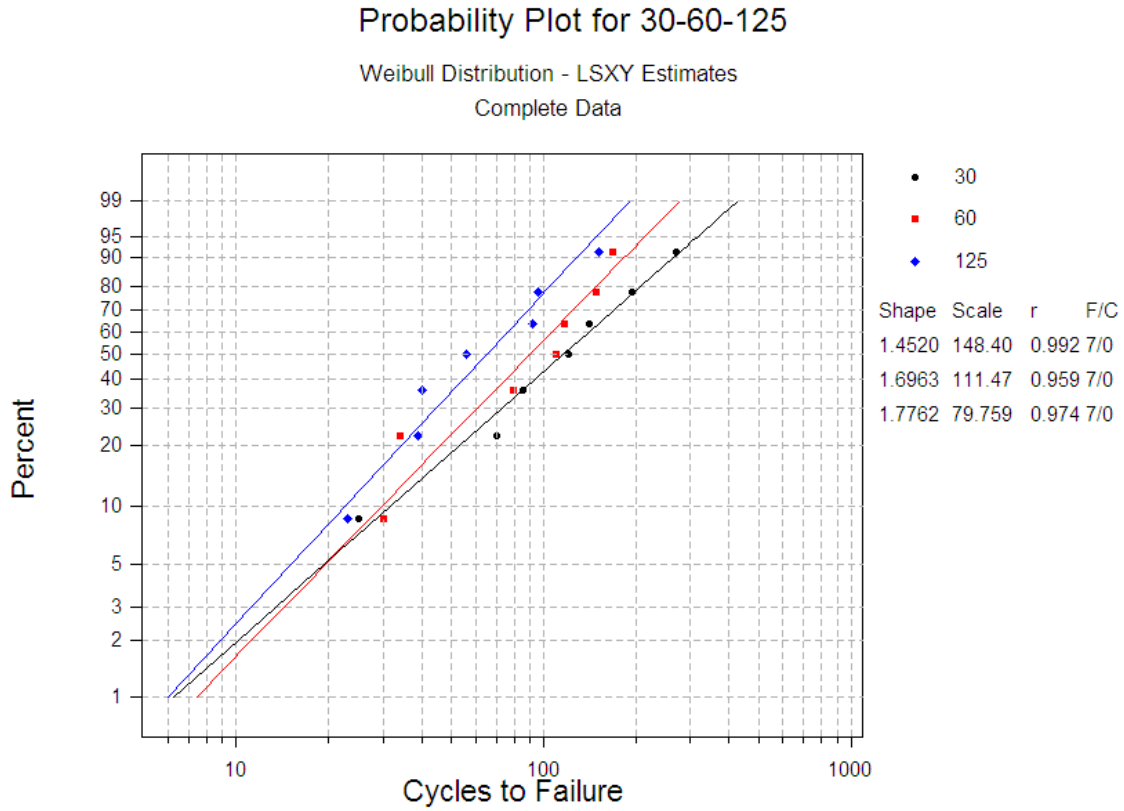


Figure 10: Lifetime degradation of SAC305 tested isothermally at 30, 60 and 125°C, for ±0.05 strain

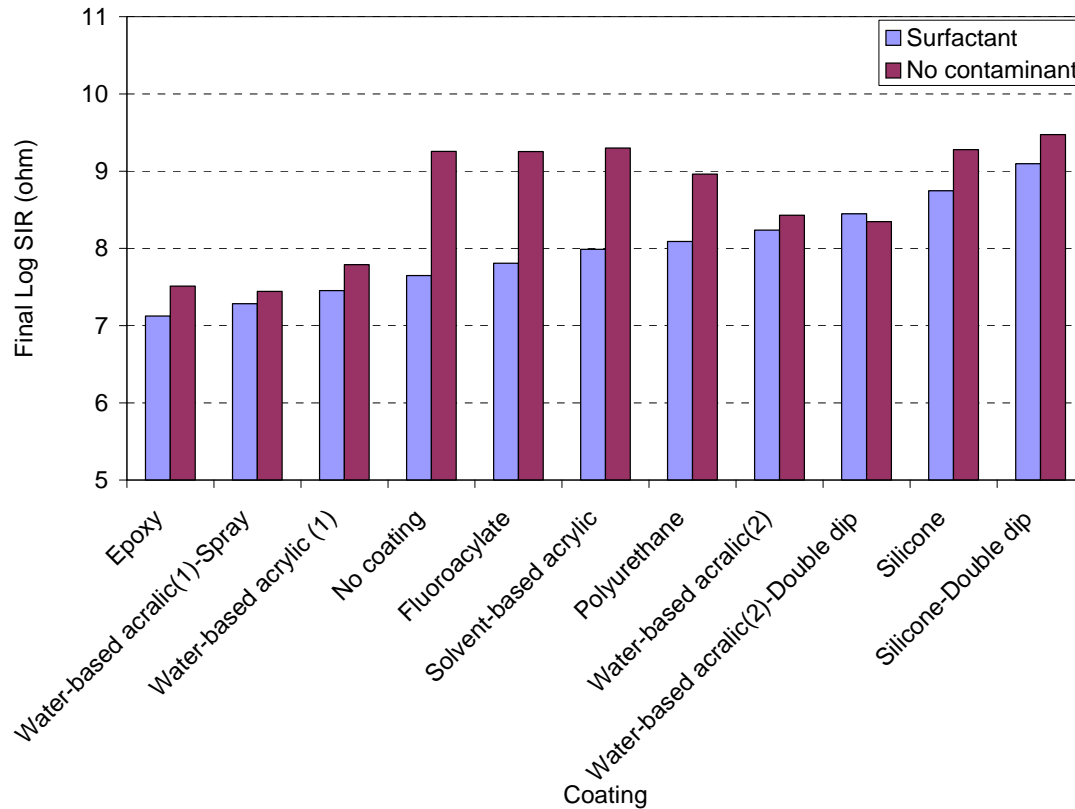


Figure 11: The relative performance of different coatings with a surfactant contaminant

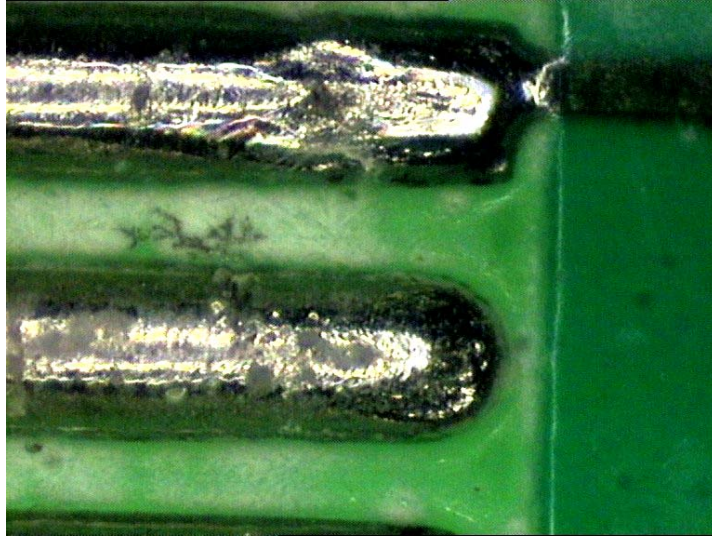


Figure 12: A dendrite forming on top of the coating

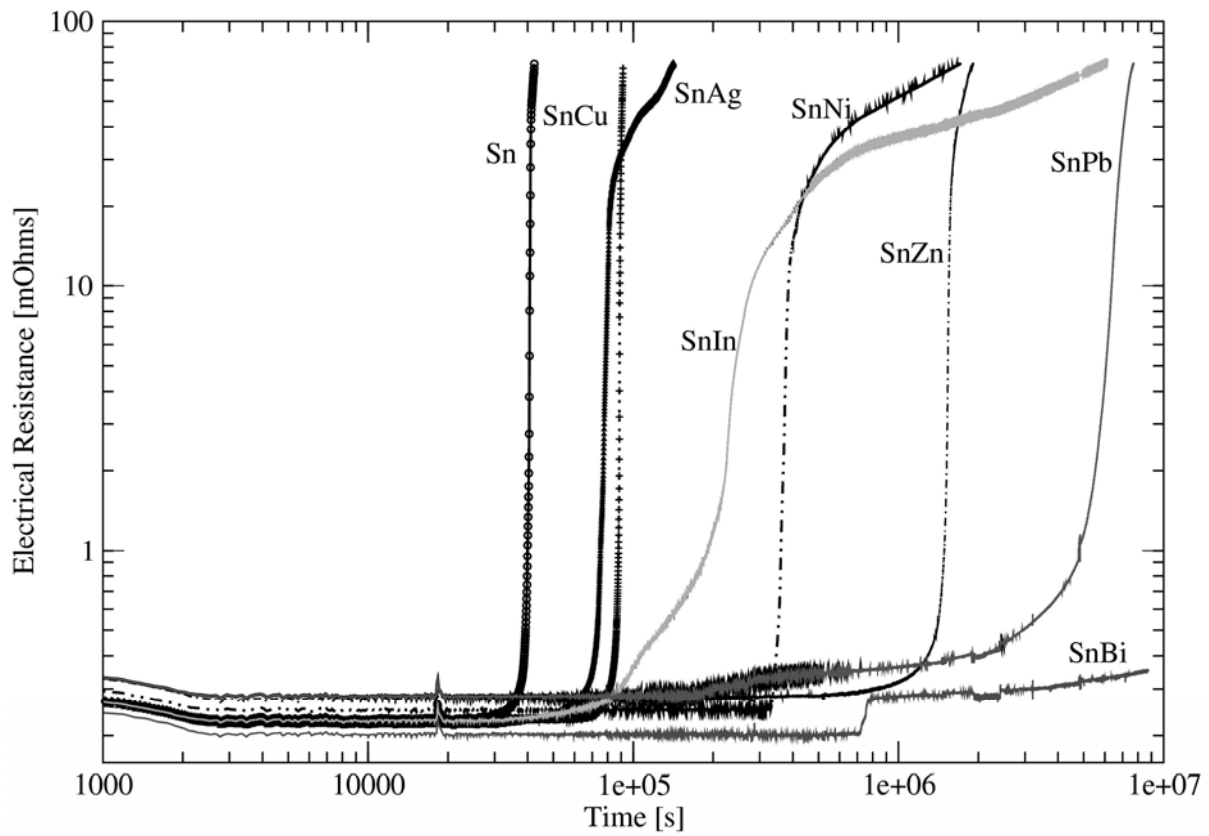
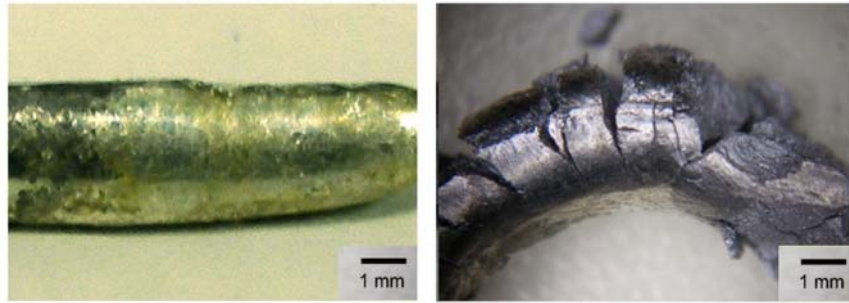


Figure 13: Electrical resistance change of Sn alloys during the transformation at -35°C.



**Figure 14: Photos of a simple hybrid Sn-Ni sample before and after the transformation. The second photograph was taken after storing the sample for approximately 1 month at  $-35^{\circ}\text{C}$ .**